STRESS ANALYSIS AND EXPANSION OF PLASTIC ZONE COMPOSITE LAMINATED PLATES ($[\theta^0/-\theta^0]_2$) UNDER TRANSVERSE LOADS BY MEANS OF FEM

Tamer ÖZBEN[*]
Nurettin ARSLAN[**]

Abstract: The aim of this work is to predict the expansion of the plastic zone and residual stresses in layers of stainless steel woven fiber-reinforced thermoplastic matrix composite laminated plates ($[\theta^0/-\theta^0]_2$) with rectangular hole. The elastic and elastic-plastic stresses are analyzed by using FEM by means of a developed computer program with FORTRAN 90. The laminated plates arranged in ($[\theta^0/-\theta^0]_2$) configuration under uniform transverse loading are formed by stacking four composite layers bonded symmetrically or antisymmetrically. Loading is gradually increased from yield point of the plate as 0.0001 Mpa at each load step. The elastic, elastic-plastic and residual stress components and the expansion of the plastic zones are obtained according to the load steps, different orientation angles and rectangular hole dimensions under clamped and simply supported boundary conditions. Results showed that the maximum stress levels and the plastic zones appear the vicinity of the rectangular hole at the upper and lower layers.

Key Words: Residual Stress, Plastic Zone, Elastic-Plastic Stress, Thermoplastic Laminated Plates, Fem.

Düşey Yükleme Altında Kompozit Tabakalı Bir Plakanın ($[\theta^0/-\theta^0]_2$) Sonlu Elemanlar Yöntemi ile Plastik Bölge Genişlemesinin ve Oluşan Gerilmenin Analizi

Özet: Bu çalışmada amaç çelik örgü fiber takviyeli termoplastik matrisli tabakalı kompozit plakanın plastik bölge dağılımını ve artık gerilmelerini öngörmektir. Elastik, elasto-plastik gerilmeler FORTRAN 90 programında hazırlanan program kullanılarak FEM analizi gerçekleştirilmiştir. Tabakalar ($[\theta^0/-\theta^0]_2$) diziliminde ve dikdörtgen delikli olarak seçilmiştir. Simetrik ve antisimetrik olarak ve belirlenen sınır şartlarında yükleme, akma noktalarından 0.0001 MPa'lık artışlarla sağlanmıştır. Maksimum gerilme değerleri ve plastik bölge oluşumu plakanın alt ve üst yüzeylerinde ve delik kenarlarında meydana gelmiştir.

Anahtar Kelimeler: Artık gerilmeler, plastik bölge, elasto-plastik gerilmeler, termoplasik tabakalı kompozit, FEM.

1. INTRODUCTION

Fiber reinforced thermoplastic composites have become an increasingly attractive alternative to metal for many aircraft, automotive, marine constructions, electronics, railway vehicle components and applications in surgery, sport equipments. Thermoplastic matrices have an unlimited shelf life before molding, and because they can potentially be remolded by the application of heat and pressure, thermoplastic matrix composites offer the possibility of lower-cost fabrication. The advantages of thermoplastic composite materials over metals have been recognized for years.

Recent interest and increased usage of advanced fibrous composite materials have made the assesment of the effects of anisotropy on the behavior of structural elements mandatory (Karakuzu, 1996). The designer has to be able to account not only for given loading but also for the directional stiffness requirements by changing the orientation angles of fibers and by arranging the stacking sequences in the laminated plates composed of two (or more) layers.

[*] Mechanical Engineering Department, Dicle University, Diyarbakır, Turkey.
[**] Mechanical Engineering Department, Balıkesir University, Balıkesir, Turkey.

It is inevitable to meet with discontinuities such as rectangular hole in the machine components made of laminated composite plates. For example, the fiber reinforced plastic laminated plate for use in train ceilings, floors and doors with rectangular holes and windows. The applications in the reinforced laminated plates have diversified to include components as varied as decor panels, structural floor panels for fast ships, performance boats and ceiling, side wall panels, partitions, landing gear doors for civil aircraft etc.

The discontinuities in the cross-sections of the members such as the laminated plate with rectangular hole give rise to stress concentration and the plastic deformation take place beyond their yield limit. Such plastic deformations cause strain hardening and redistribution of localized stress concentrations to result in an increase of the failure resistance of the members. The obtaining of the residual stresses and plastic zones appearing in the reinforced thermoplastic-matrix laminated plates are very important in failure analysis. The obtained residual stresses can be used to raise the yield points of the plates. Prediction and measurement of the plastic zones and residual stresses are also important in relation to production, design, and performance of composite components (Arslan and et al., 2004). Elastic-plastic stress analysis in thermoplastic composite laminated plates under in-plane loading was carried out by Özcan; yield points and stresses were obtained for symmetric and antisymmetric laminated plates with or without a hole (Özcan, 2000). In a similar paper, Atas and Sayman have investigated elastic-plastic stress analysis and expansion of plastic zone in clamped and simply supported aluminum metal-matrix laminated plates (Ataş and Sayman, 2000). Eijpe and Powell (1997) investigated residual stress evaluation in composite using a modified layer removal method. In the other study, the analysis of elasto-plastic stress in the aluminum metal-matrix composite laminate with a circular hole subjected to in-plane loads by means of FEM was performed (Özbay and Özer, 2005). In the relevant paper, the laminated plates were unidirectionally reinforced. Alexandrova and Alexandrov have investigated elasto-plastic stress distribution in a rotating annular disk. The analysis was based on the Mises yield criterion and its associated flow rule. The radius of elastic-plastic boundary was found as a function angular velocity (Alexandrova and Alexandrova, 2004). Eraslan and Akgün (2005) studied yielding and elastoplastic deformation of annular disks of a parabolic section subjected to external compression. The model is based on the von Mises' yield criterion, deformation theory of plasticity and Swift type hardening law. Arslan and Özben presented an elastic-plastic stress analysis in a unidirectional reinforced steel fiber thermoplastic cantilever beam loaded by a single force at the free end [Arslan and Özben, 2005). Sayman et al. (2002) have investigated thermal elastic-plastic stress analysis of symmetric aluminum metal-matrix composite laminated plates under uniformly distributed temperature. The composite material was assumed strain-hardening lineraly. The magnitude of the residual stress components in the cross-ply laminated plate was higher than in the angle-ply laminated plates. Neumann et al. (2001) carried out a study of Furier transformation an alternative to finite elements for elastic-plastic stress-strain analyses of heterogeneous materials. There have been many studies about predicting expansion of plastic zone and calculating elastic, plastic, and residual stresses for fiber reinforced laminated composite plates (12-21).

This paper focuses on determining the elastic, plastic, and residual stresses and on predicting the plastic zone growth in layers of stainless steel woven fiber-reinforced thermoplastic matrix composite laminated plates with rectangular hole (Fig. 1). The layers in the laminated plate arranged in $[\theta^0/-\theta^0]_2$ are oriented $[0^0/0^0]_2$, $[15^0/-15^0]_2$, $[30^0/-30^0]_2$, and $[45^0/-45^0]_2$. The Tsai-Hill theory is used as a yield criterion. The relevant analysis is carried out by FEM (a nine-node isoparametric quadrilateral element) and first-order shear deformation theory under clamped and simply supported boundary conditions for symmetric and antisymmetric lamination. The uniform transverse loading for small deformation is increased by 0.0001 MPa increments at each iteration choosen as 25, 50, 75 and 100. At the end of the given analysis, elastic, elastic-plastic, and residual stresses are calculated and the spread of the plastic zone with respect to rectangular hole dimensions, increasing loads, lamination types and different orientation angles, stacking sequences, and various composite materials.

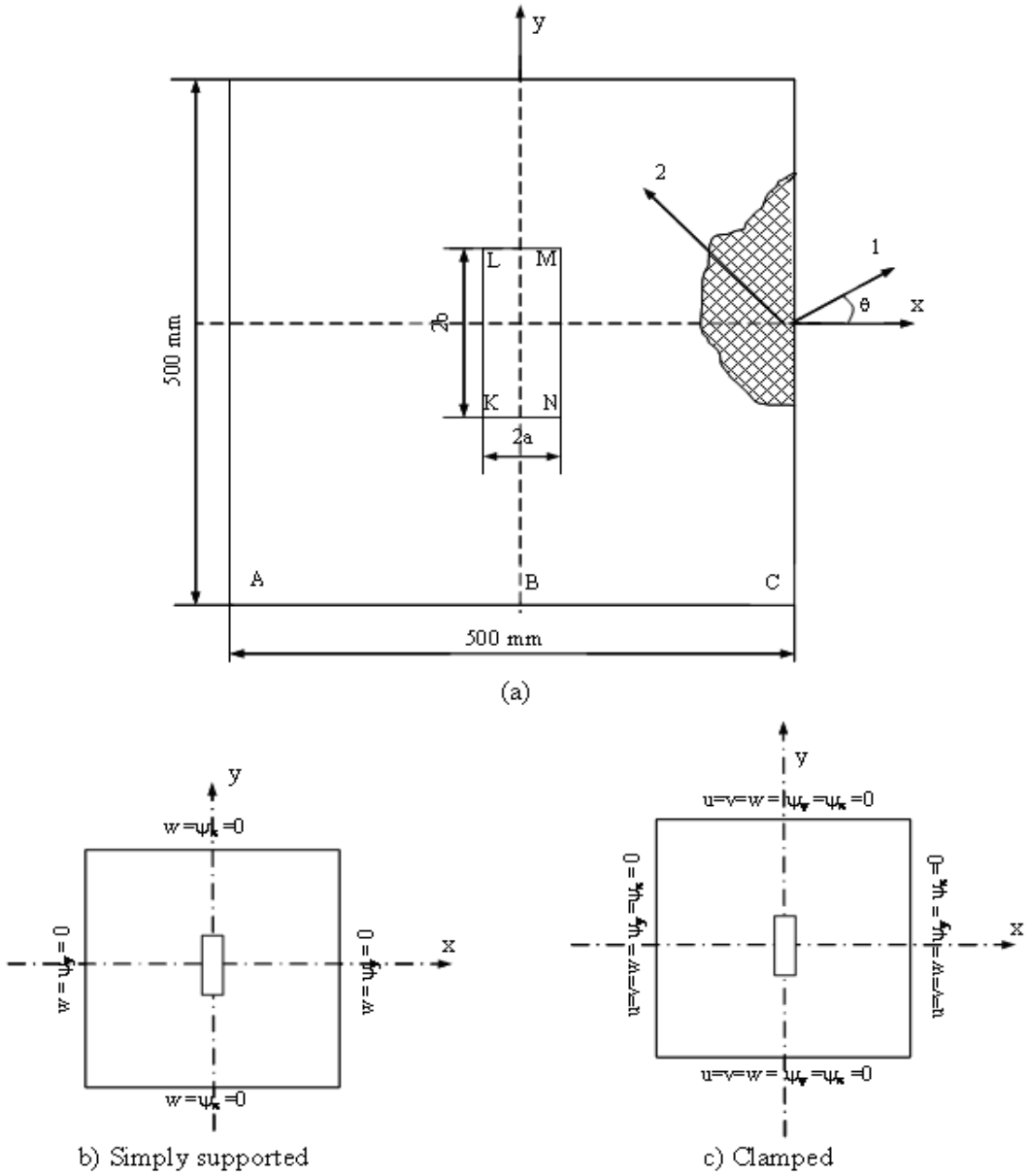

Figure 1:
Geometry (a) boundary conditions (b,c) of the loaded plate with rectangular hole in cartesian coordinates for simply supported and clamped supports, respectively.

2. MATHEMATICAL FORMULATION

The woven stainless steel fiber reinforced thermoplastic-matrix laminated plates are of four orthotropic layers with constant thickness, 2.1 mm. The plates are composed of orthotropic layers bonded symmetrically or antisymmetrically about the middle surface of the plate. The laminated plates are loaded with clamped and simply supported boundary conditions illustriated in Fig.2. In these figures, the middle surface of the plate coincides with x-y plane. The Cartesian coordinates are used in the solution. Consider transverse shear deformations in the solution of laminated plate elements (Bahei El-Din and Dovark, 1982) the stress-strain relations associated with the xyz-axes for an orthotropic layer in any reinforcement angle can be written as below [23].

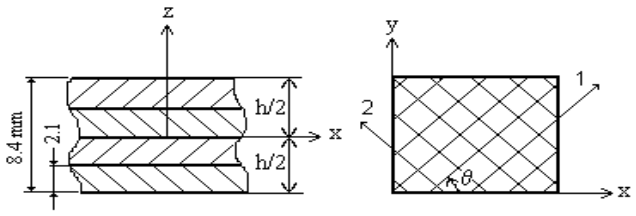

Lamination of the model

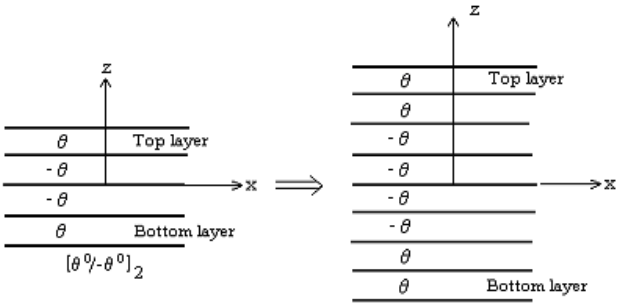

A typical laminated plate divided into 8 imaginary layers.

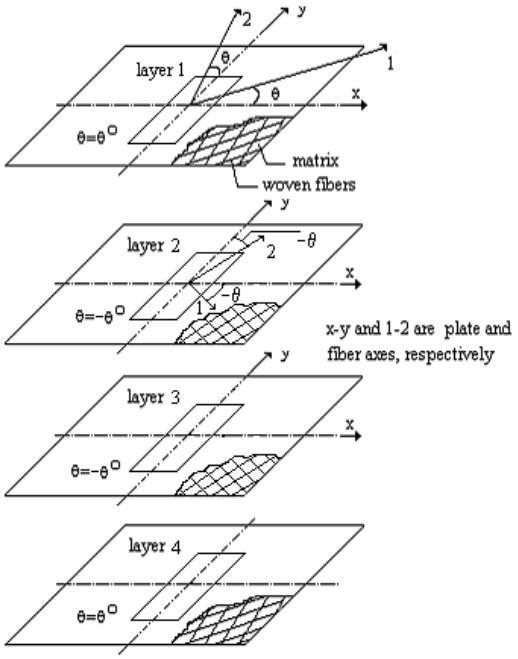

(c) $[\theta^0/-\theta^0]_2$ orientation type of the woven cross-ply reinforced layers.

Figure 2:
A layered section for symmetric lamination.

$$\begin{Bmatrix}\sigma_x\\ \sigma_y\\ \tau_{xy}\end{Bmatrix}_k = \begin{bmatrix}\overline{Q}_{11} & \overline{Q}_{12} & \overline{Q}_{16}\\ \overline{Q}_{21} & \overline{Q}_{22} & \overline{Q}_{26}\\ \overline{Q}_{61} & \overline{Q}_{62} & \overline{Q}_{66}\end{bmatrix}_k \begin{Bmatrix}\varepsilon_x\\ \varepsilon_y\\ \gamma_{xy}\end{Bmatrix}_k$$

$$\begin{Bmatrix}\tau_{yz}\\ \tau_{xz}\end{Bmatrix}_k = \begin{bmatrix}\overline{Q}_{44} & \overline{Q}_{45}\\ \overline{Q}_{54} & \overline{Q}_{55}\end{bmatrix}_k \begin{Bmatrix}\gamma_{yz}\\ \gamma_{xz}\end{Bmatrix}_k \qquad (1)$$

where subscribt k refers to the *i*th lamina, $\overline{Q}_{ij}$ are the transformed reduced stiffnesses and can be defined in terms of engineering constants of material C_{ij} (or D_{ij}) and orientation angle, θ. The first-order shear deformation theory was used. According to this theory, normals to the middle surface remain straight and normal during deformation (Gibson, 1994). With this assumption the displacement for small deformations can be expressed as

$$\begin{aligned} u(x,y,z) &= u_0(x,y) + z\,\psi_x(x,y) \\ v(x,y,z) &= v_0(x,y) - z\,\psi_y(x,y) \\ w(x,y) &= w_0(x,y) \end{aligned} \tag{2}$$

where u_0, v_0 are the tangential displacements of the middle surface along the x and y directions, respectively. z is the distance from neutral surface defined by the xy plane. Due to the transverse normal strain ε_z is negligible, the transverse displacement at the middle surface, $w_0(x,y)$, is the same as the transverse displacement of any point having the same x and y coordinates, so $w(x,y) = w_0(x,y)$. ψ_x and ψ_y denote rotations about the normal to the y- and x- axes, respectively. Here $\psi_x = -\partial w/\partial x$, $\psi_y = \partial w/\partial y$ with respect to its followed variables. As given below, the bending strains vary linearly through the plate thickness,

$$\begin{Bmatrix} \varepsilon_x \\ \varepsilon_y \\ \gamma_{xy} \end{Bmatrix} = \begin{Bmatrix} \dfrac{\partial u_0}{\partial x} \\ \dfrac{\partial v_0}{\partial y} \\ \dfrac{\partial u_0}{\partial y} + \dfrac{\partial v_0}{\partial x} \end{Bmatrix} + z \begin{Bmatrix} \dfrac{\partial \psi_x}{\partial x} \\ -\dfrac{\partial \psi_y}{\partial y} \\ \dfrac{\partial \psi_x}{\partial y} - \dfrac{\partial \psi_y}{\partial x} \end{Bmatrix} \quad \text{or}$$

$$\begin{Bmatrix} \varepsilon_x \\ \varepsilon_y \\ \gamma_{xy} \end{Bmatrix} = \begin{Bmatrix} \varepsilon_x^0 \\ \varepsilon_y^0 \\ \gamma_{xy}^0 \end{Bmatrix} + z \begin{Bmatrix} K_x \\ K_y \\ K_{xy} \end{Bmatrix} \tag{3}$$

whereas shear strains are assumed to be constant through the thickness as,

$$\begin{Bmatrix} \gamma_{yz} \\ \gamma_{xz} \end{Bmatrix} = \begin{Bmatrix} \dfrac{\partial w}{\partial y} - \psi_y \\ \dfrac{\partial w}{\partial x} + \psi_x \end{Bmatrix} \tag{4}$$

The total potential energy of a laminated plate under static loading is written as,

$$\Pi = U_b + U_s + V \tag{5}$$

where U_b, and U_s are bending and shear terms of internal energy, respectively and V is also the potential energy of external forces. These values are given as

$$U_b = \frac{1}{2} \int_{-\frac{h}{2}}^{\frac{h}{2}} \left[\int_A \left(\sigma_x \varepsilon_x + \sigma_y \varepsilon_y + \tau_{xy} \gamma_{xy} \right) dA \right] dz$$

$$U_s = \frac{1}{2} \int_{-\frac{h}{2}}^{\frac{h}{2}} \left[\int_A \left(\tau_{xz} \gamma_{xz} + \tau_{yz} \gamma_{yz} \right) dA \right] dz \tag{6}$$

$$V = -\int_A w.p.dA - \int_{\partial R} \left(\overline{N}_n^b \, u_n^0 + \overline{N}_s^b \, u_s^0 \right) ds$$

where dA=dx.dy, h is the total thickness of the plate, p is the transverse loading per unit area and $\overline{N}_n^b$ and $\overline{N}_s^b$ are the in-plane forces per unit length acting on the boundary ∂R.

In the laminated plate analysis, however, it is convenient to use forces and moments per unit length referred to as stress resultants rather than forces and moments. The mentioned stress resultants are

$$\begin{Bmatrix} N_x , M_x \\ N_y , M_y \\ N_{xy} , M_{xy} \end{Bmatrix} = \int_{-\frac{h}{2}}^{\frac{h}{2}} \begin{Bmatrix} \sigma_x \\ \sigma_y \\ \tau_{xy} \end{Bmatrix} (1, z) \, dz ,$$

$$\begin{Bmatrix} N_{xz} \\ N_{yz} \end{Bmatrix} = \begin{Bmatrix} Q_x \\ Q_y \end{Bmatrix} = \int_{-\frac{h}{2}}^{\frac{h}{2}} \begin{Bmatrix} \tau_{xz} \\ \tau_{yz} \end{Bmatrix} dz \tag{7}$$

For static equilibrium, Π is stationary or a minimum, that is the second variation of Π is positive at the stationary point, i.e., or δΠ=0 for equilibrium. It may be regarded as the principle of virtual displacements for the plate (Bathe, 1982).

3. ELASTO-PLASTIC SOLUTION

In the elastic-plastic solution, strain increment are given by $\{d\varepsilon\} = \{d\varepsilon_e\} + \{d\varepsilon_p\}$, where $\{d\varepsilon_e\}$ and $\{d\varepsilon_p\}$ are the elastic and plastic components of the strain increments, respectively. The laminated composite material is strain hardening. If the material strain hardens it is usual to assume that the size of the yield surface increase. The plastic increments occur normal to the yield surface. Thus the progression past the yield surface $d\sigma_p^*$ is given by (Mohr, 1992)

$$d\sigma_p^* = \left\{ \frac{\partial f}{\partial \sigma} \right\}^T .\{d\sigma\} = F^T .\{d\sigma\} \tag{8}$$

where $f(\{\sigma\})$ defines the equivalent uniaxial stress σ_e (or σ^*) and, as it is obtained from the Tsai-Hill yield criterion. The multiaxial case is reduced to a uniaxial case by using the effective or equivalent stress, σ_e. The elasto-plastic stress analysis is performed when the equivalent stress exceeds the yield strength of the material.

The mechanical properties consisting of yield points and plastic parameters and etc. of a layer for material produced by heating press designed at the Firat University Mechanical Laboratory were obtained experimentally from measured values found by using strain gages as shown in the literature and are given in Table I. The mechanical tests and measurements according to the relevant ASTM standards were realised in the Mechanical laboratories of Dokuz Eylul and Firat Universities by using electromechanical test systems (Instron and Utest, respectively) and strain indicator with data acquisition (Measurements Group-Strain indicator P-350A, Iotech DBK43A and DaqBoard/2000). There is no debonding between fiber and matrix. It is sufficient to measure longitudinal (X) and transverse (Y) tensile strengths of woven lamina; Young's moduli, E_1 and E_2; and Poisson's ratio ν_{12} by only testing longitudinal (0^0) specimens, since specimens are woven. Because of the woven lamina, it is obvious that E_1, and X are equal to E_2, and Y, respectively. These properties and shear strength, S given in Table I had been measured in the study by using strain gages which are bonded on the specimens in longitudinal, transverse, and 45^0 directions. It is assumed that the yield point, in the z direction, Z is equal to the yield point Y, in the y direction. The yield points of τ_{xz}, τ_{yz} are assumed to be equal to S which is the yield point of τ_{xy}. Because of the reinforcing steel fibers, the composite layer possesses

the same yield points in tension and compressions for numerical solution. Thus according to the Tsai-Hill theory,

$$\sigma_e^2 = \sigma_1^2 - \sigma_1\sigma_2 + \sigma_2^2 \left(\frac{X^2}{Y^2}\right) + (\tau_{12}^2 + \tau_{13}^2 + \tau_{23}^2)\left(\frac{X^2}{S^2}\right) = X^2 \quad (9)$$

where σ_1, σ_2,τ_{12},τ_{13} and τ_{23} are the stress components in the principal material directions. The yield function f is,

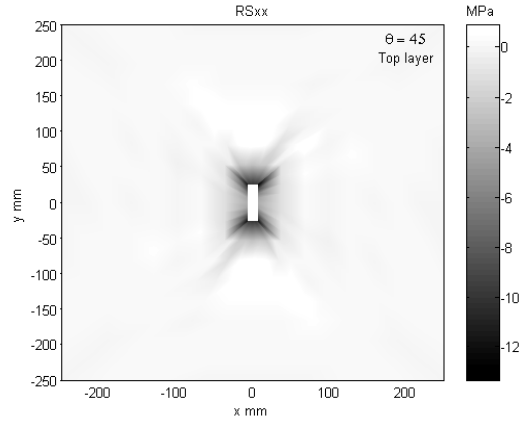

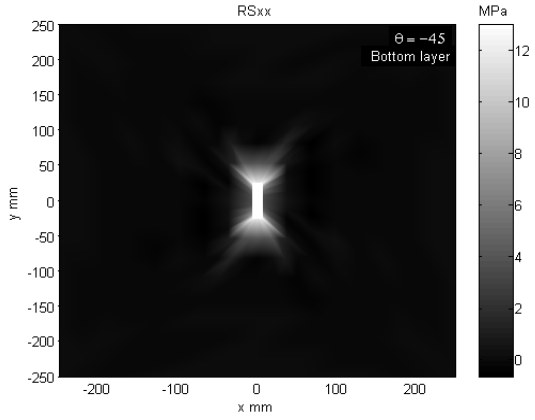

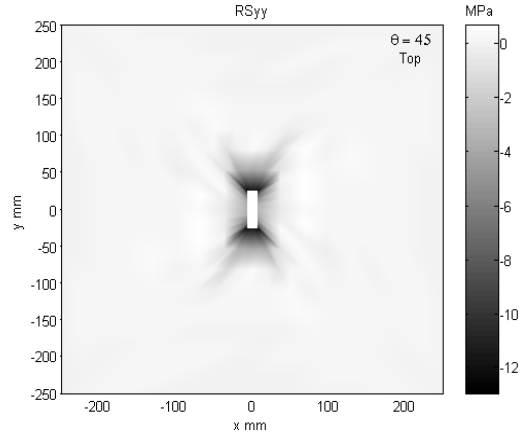

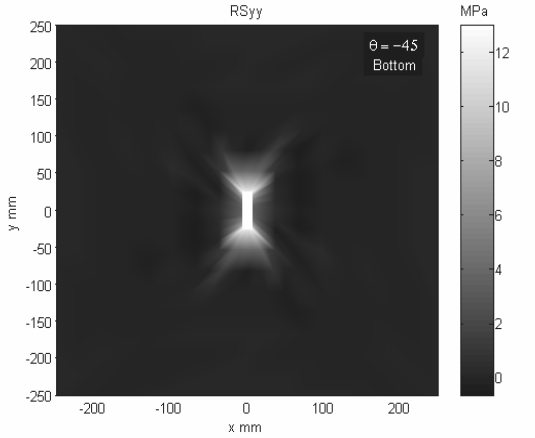

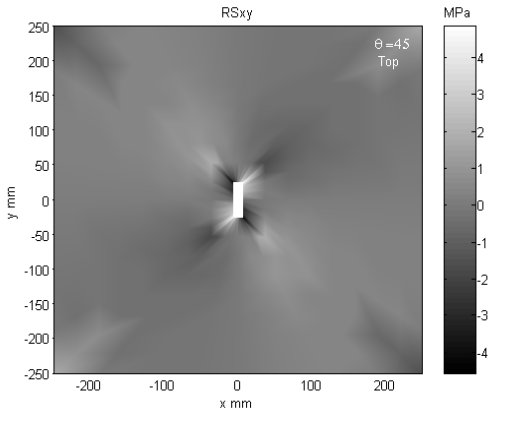

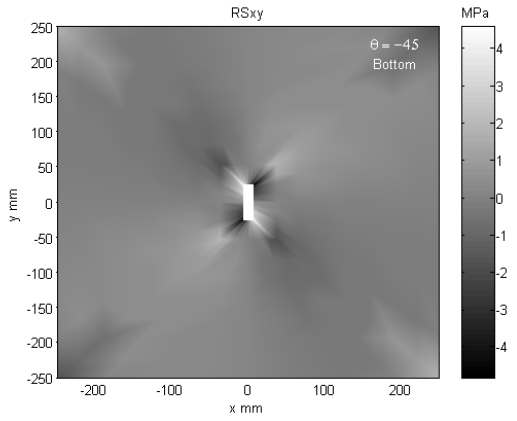

Figure 3:
Mapping of residual stresses components on the upper surface ((θ=45^0) for antisymmetric simply supported laminated plate ([45^0/-45^0]$_2$) and 100 load steps.

Figure 4:
Mapping of residual stresses components on the lower surface ((θ=45^0) for antisymmetric simply supported laminated plate ([45^0/-45^0]$_2$) and 100 load steps.

$$f = \sigma_e - X = \sigma_e - \sigma_0 = 0 \tag{10}$$

where σ_0 is the yield stress (Mohr, 1992).

$$f(\sigma_x, \sigma_y, ,\tau_{xy}, \tau_{xz}, \tau_{yz}) = [\sigma_x^2 - \sigma_x\sigma_y + \sigma_y^2 \left(\frac{X^2}{Y^2}\right) + (\tau_{xy}^2 + \tau_{xz}^2 + \tau_{yz}^2) \left(\frac{X^2}{S^2}\right)]^{1/2} \tag{11}$$

and when the numerical value of this, the equivalent uniaxial stress σ^*, equals or exceeds X, yielding occurs. The rate of progression past the yield surface $d\sigma_p^*$ can be calculated using a plastic flow law obtained by chain differentiation of the yield function f of equ (11) giving

$$F = \left\{2\sigma_x - \sigma_y, 2\sigma_y \frac{X^2}{Y^2} - \sigma_X, 2\tau_{xy} \frac{X^2}{S^2}, 2\tau_{xz} \frac{X^2}{S^2}, 2\tau_{yz} \frac{X^2}{S^2}\right\} \Big/ 2\sigma_e \tag{12}$$

One can write by using the elasticity matrix

$$\{d\sigma\} = D.\{d\varepsilon\} - D.\{d\varepsilon_p\} \tag{13}$$

Using eqn (8) the following equation can be obtained

$$d\sigma_p^* == F^T.D.\{d\varepsilon\} - F^T.D.\{d\varepsilon_p\} \tag{14}$$

A hardening rule based on uniaxial behaviour is introduced (Johnson, 1983),

$$d\sigma_p^* = H.d\varepsilon_p^* \tag{15}$$

where H is the slope of the uniaxial stress-plastic strain curve in the plastic range. Assuming also an associated flow rule for the plastic strain increments:

$$\{d\varepsilon_p\} = F.d\varepsilon_p^* \tag{16}$$

where $d\varepsilon_p^*$ corresponds to $d\sigma_p^*$. This is referred to as the Prandtl-Reuss flow rule. A symmetric tangent modulus matrix, D_T, is obtained by using (13)-(16),

$$D_T = D - \frac{D.F.F^T.D}{H + F^T.D.F} \tag{17}$$

This replaces the elastic modulus matrix, D, when $\sigma_{e_i} \geq \sigma_o$ in the load increment i.

4. LOAD STEPPING TECHNIQUES

In this study, the used iterative solution can be derived from the Newton-Raphson method. The simplest approach to the analysis of nonlinear problems in FEM is load stepping with the total load $\{R_n\} = \sum \{\delta R_i\}$, being built up in a series of steps $i = 1 \rightarrow n$. Then the displacement solution after application of the *i*th load increments is obtained as

$$\{U\}_{i+1} = \{U\}_i + K_T^{-1}.\{\delta R_i\} \tag{18}$$

where K_T is tangential stiffness matrix. In addition, K_T and $\{R\}$ are calculated using the displacements $\{U\}_i$, this process is repeated. This is often referred to as Euler's method. For a linear extrapolation along a tangent, Euler's formula gives

$$\varepsilon_{i+1} = \varepsilon_i + \frac{\delta\sigma}{\left(d\sigma \big/ d\varepsilon\right)_i} \tag{19}$$

where σ is stress-strain relation in plastic region, and is given by Ludwik's empirical expression as,

$$\sigma = \sigma_o + k.\varepsilon_p^n \tag{20}$$

where σ_o is equal to X which is the yield point in the first principal material direction, k, ε_p and n are the plasticity constant, equivalent plastic strain, and strain hardening exponent, respectively. In addition, the empirical curves [26] for σ in Eq.20. (If the strain hardening exponents, n, changing from 0 to 1, have 0 and 1 values the materials are called ideal plastic and ideal elastic, respectively. The mentioned material properties were attained experimentally from the load-displacement diagram.

5. FINITE ELEMENT ANALYSIS

In this study, a nine-node Lagrangian finite element is used to acquire the first yield point, the residual stresses, and the spread of the plastic zone of the laminated composite plates with rectangular hole for all selected materials. In this analysis, the symmetric and antisymmetric laminated plates are composed of four layers. The plates are divided into eight imaginary parts (Fig.2) for obtaining the results more accurately. The laminated plates are loaded transversely with simply supported and clamped boundary conditions shown in Fig.1 where the middle surface of the plate coincides with the xy plane. In the FEM solution, each layer in the laminated plate having geometric and loading symmetry is automatically meshed into 64 element 288 nodes to compare with the obtained values and the literature values more accurately. The displacement field can be expressed in the following matrix form as,

$$[d]=\begin{bmatrix} u_0 \\ v_0 \\ w \\ \psi_x \\ \psi_y \end{bmatrix}=\sum_{i=1}^{n}\begin{bmatrix} N_i & 0 & 0 & 0 & 0 \\ 0 & N_i & 0 & 0 & 0 \\ 0 & 0 & N_i & 0 & 0 \\ 0 & 0 & 0 & N_i & 0 \\ 0 & 0 & 0 & 0 & N_i \end{bmatrix}\begin{bmatrix} u_0 \\ v_0 \\ w \\ \psi_x \\ \psi_y \end{bmatrix} \tag{21}$$

where N_i is the shape function at the node i and n is the total number of nodes in the FE model. The relationship between strain-displacement can be expressed in Eq.(2) and (23), respectively, by using Eq.(3) symbolically as,

$$\{\varepsilon_{bi}\}=[B_{bi}]\{u_i\} \tag{22}$$

$$\{\varepsilon_{si}\}=[B_{si}]\{u_i\} \tag{23}$$

where i is the node number and [B] is the transformation matrix. The final form of the element stiffness matrix of the plate element is obtained by using the minimum potential energy method of the principle of virtual displacements. Bending and shear stiffness are obtained as,

$$[K_b]=\int_A [B_b]^T[D_b][B_b]dA$$

$$[K_s]=\int_A [B_s]^T[D_s][B_s]dA \tag{24}$$

where,

$$[D_b]=\begin{bmatrix} A_{ij} & B_{ij} \\ B_{ij} & D_{ij} \end{bmatrix}, \qquad [D_s]=\begin{bmatrix} k_1^2A_{44} & 0 \\ 0 & k_2^2A_{55} \end{bmatrix}$$

$$(A_{ij},B_{ij},D_{ij})=\int_{-\frac{h}{2}}^{\frac{h}{2}} Q_{ij}(1,z,z^2)dz \qquad (i=j=1,2,6)$$

$$(A_{44},A_{55})=\int_{-\frac{h}{2}}^{\frac{h}{2}} (Q_{44},Q_{55})dz \tag{25}$$

where D_b and D_s are the elasticity matrices of bending and shear parts of the material matrix, respectively. A_{45} is negligible in comparison with A_{44} and A_{55}. k_1 and k_2 denote the shear correction factors for rectangular cross sections and are given as $k_1^2 = k_2^2 = 5/6$ [4,27].

In this work, two dimensional plate element is used instead of 3D plate element because of the plate thickness being very small. Although the displacements in z-axis, w, are taken into consideration for 2D plate analysis. In this solution, the external forces are applied transversely and are increased incrementally. For the non-linear stress analysis, the unbalanced nodal forces and the equivalent nodal forces must be calculated for each load step. The equivalent nodal forces at each load step can be calculated as given below,

$$\{R\}_{\text{equivalent}} = \int_{\text{vol}} [B]^T \{\sigma\}.dA = \int_{\text{vol}} [B_b]^T \{\sigma_b\}.dA + \int_{\text{vol}} [B_s]^T \{\sigma_s\}.dA \tag{26}$$

The unbalanced nodal forces can be obtained, because the equivalent nodal forces are known. It gives,

$$\{R\}_{\text{unbalanced}} = \{R\}_{\text{applied}} - \{R\}_{\text{equivalent}} = K_T.\{\delta U\} \tag{27}$$

In the non-linear solution, the obtained unbalanced nodal forces are applied for obtaining increments by the modified Newton Raphson method [19]. The difference between the elastic-plastic and elastic stresses gives the residual stress, RS ($=\tau^I$). The residual stress load vector, $\{R\}_I$, is added to the total external applied load vector $\{R\}$.

The stress concentrations can be reduced through the residual stresses. Thus the failure of the laminated plate may be delayed and the load capacity of the plate increases by the residual stresses.

6. RESULTS AND DISCUSSIONS

An elastic-plastic stresses analysis is accomplished in the clamped and simply supported laminated plates with rectangular hole under uniform transverse static loads for $[\theta^0/-\theta^0]_2$ stacking sequence. The determinations of elastic-plastic solution and the plastic region distribution are completed by using symmetric and antisymmetric thermoplastic laminated plates made up four layers. The transverse load was increased to 0.0001 MPa at each load step from the yield point of the plate of different orientation angles and different supports cases. The load steps were chosen as 25, 50, 75 and 100 for clamped and simply supported cases.

The uniform transverse forces at the yield points of both cases are shown in Table II. It is seen that the yield points of the symmetric stacked plates are higher than those of antisymmetric stacked plates at $[15^0/-15^0]_2$ and $[30^0/-30^0]_2$ stacking sequences for simply supported case. However, symmetric stacked plates are lower than those of antisymmetric stacked plates at $[45^0/-45^0]_2$ stacking sequence for simply supported case. The yield points of the symmetric stacked plates are higher than those of antisymmetric stacked plates at $[15^0/-15^0]_2$ stacking sequence for clamped case. The relevant values for $[0^0/0^0]_2$, $[30^0/-30^0]_2$ and $[45^0/-45^0]_2$ stacking sequences are same for clamped case. The yield points of the symmetric and the antisymmetric laminated clamped plates are, it is observed, higher than those of simply supported plates.

Table III provides the maximum elastic and residual stress components at the corner of the rectangular hole (point K) for all layers in clamped and simply supported laminated plates $[45^0/-45^0]_2$. The layers are stacked symmetrically and antisymmetrically and the load step is 100. It is observed that the stress values at the upper and lower layers are higher than those at inner layers for either symmetric or antisymmetric lamination due to the loading condition. The same situation can be noticed in both clamped and simply supported laminated plates. For symmetric and antisymmetric lamination, the smallest elastic and residual stress values are obtained at the layers which are the adjacent to the midplane in either clamped or simply supported plates, as expected. In addition, elastic and residual stress values at layers having same distance from the midplane are absolutely equal for either symmetric or antisymmetric lamination because of the woven reinforcement and $[45^0/-45^0]_2$ stacking sequence.

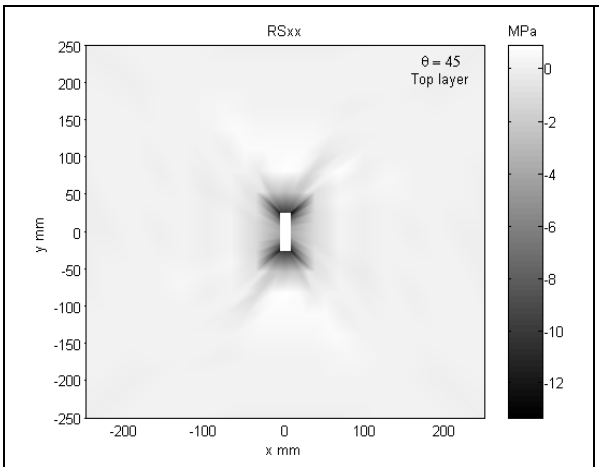

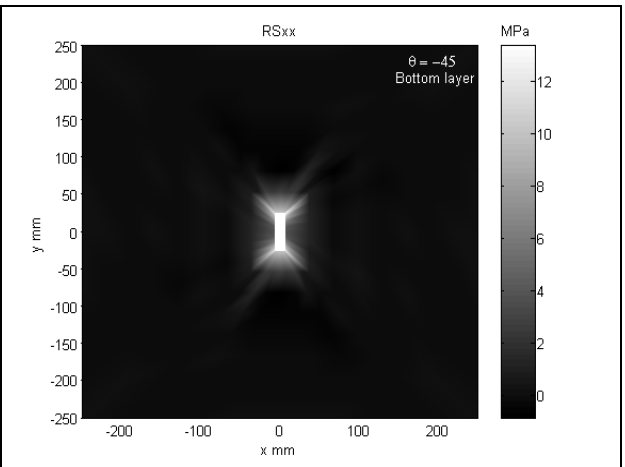

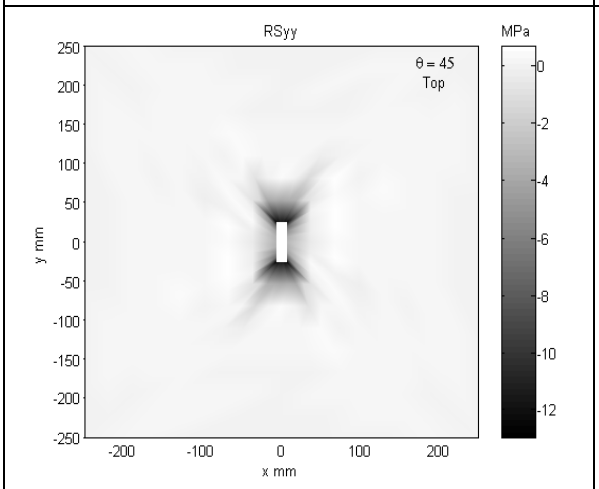

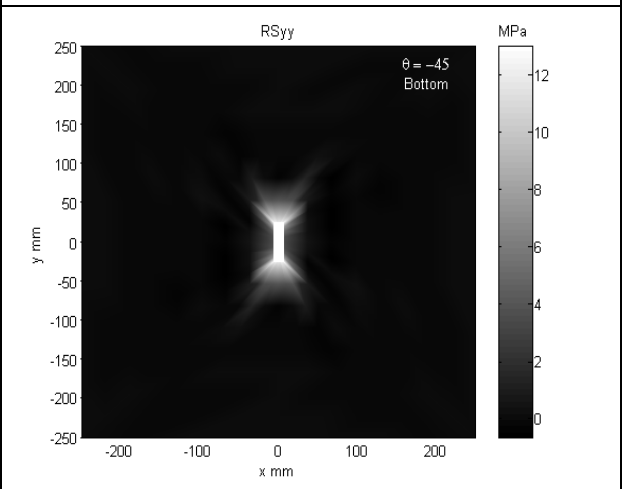

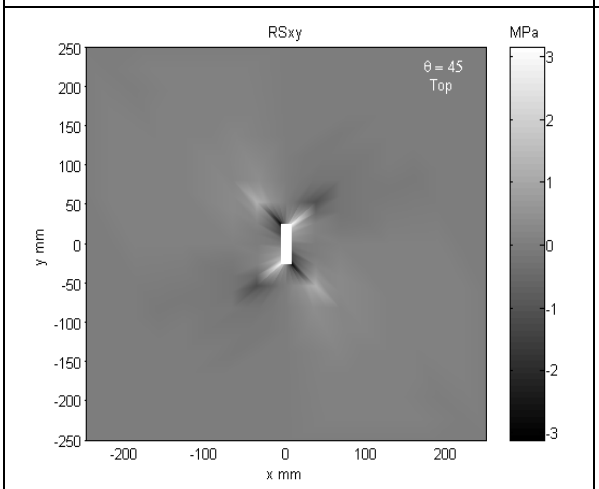

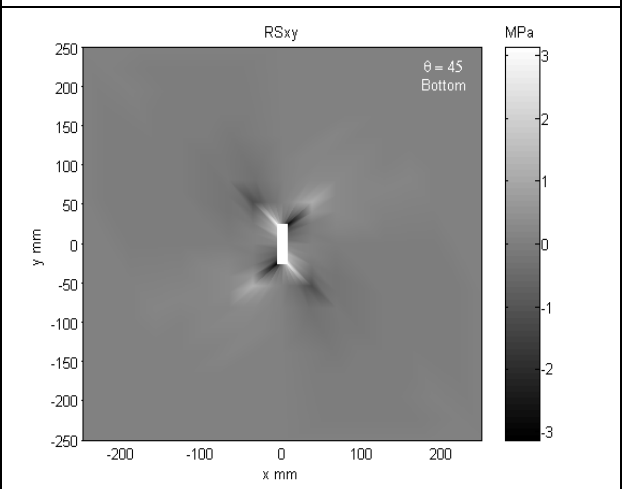

Figure 5:
Mapping of residual stresses components on the upper surface ($\theta=45^0$) for antisymmetric clamped laminated plate ($[45^0/-45^0]_2$) and 100 load steps.

Figure 6:
Mapping of residual stresses components on the lower surface ($\theta=-45^0$) for antisymmetric clamped laminated plate ($[45^0/-45^0]_2$) and 100 load steps.

The maximum stresses in clamped and simply supported cases (Table IV and V, respectively) are presented for different stacking sequence ($[\theta^0/-\theta^0]_2$) and symmetric and antisymmetric lamination at p=0.0225 and 0.01269 MPa constant loads. The variations of the fiber orientation angles are selected between +45 and -45 due to the woven reinforcement. The maximum elastic and residual stress values at $[45^0/-45^0]_2$ stacking sequence are smaller than those at $[0^0/0^0]_2$, $[15^0/-15^0]_2$ and $[30^0/-30^0]_2$ for

either symmetric or antisymmetric laminations. A similar behavior was also seen for $[0^0/\theta^0]_2$ stacking sequence. For clamped and simply supported boundary conditions, the intensity of the stress components at the upper and lower surfaces of symmetric oriented laminates are absolutely equal than those of antisymmetric case due to the $[\theta^0/-\theta^0]_2$ lamination and the woven fiber type. This result agrees with the result of literature [1,19].

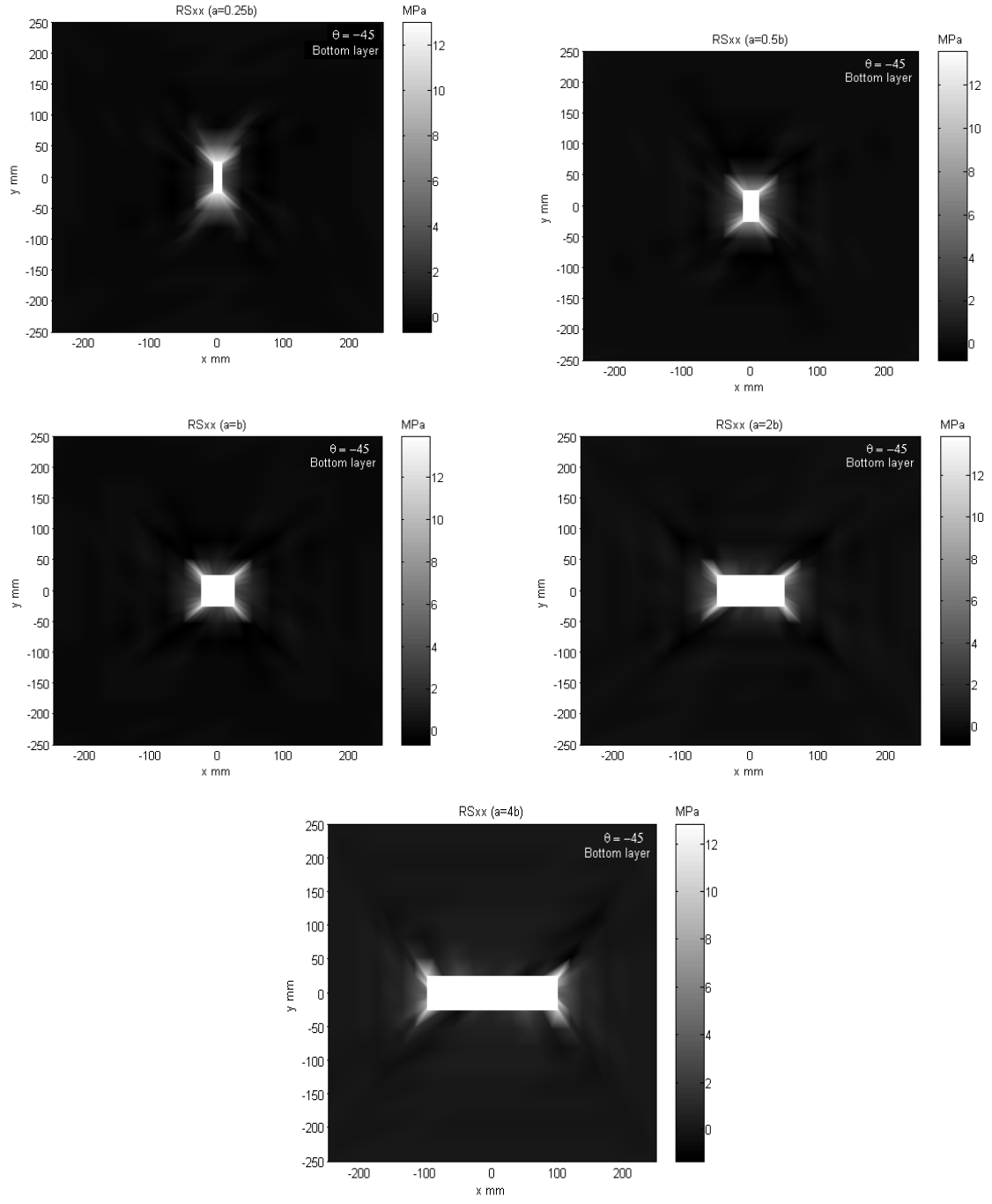

Figure 7:
Mapping of hole dimension (a,b) on the lower surface (θ=–45^0) for antisymmetric simply supported laminated plate ([45^0/-45^0]$_2$) and 100 load steps.

Figures 3, 4, 5 and 6 give plotting of the residual stress components (RS_{xx}, RS_{yy}, RS_{xy}) on the upper and lower surfaces in the antisymmetric simply supported and clamped laminated plates ([45^0/-

$45^0]_2$) for 100 load steps. For the $[\theta^0/-\theta^0]_2$ lamination, the residual stress values for simply supported case are higher than those for clamped case. The results were found to agree with the literature [1].

Fig. 7 ve Fig.8 for ($[45^0/-45^0]_2$) stacking sequence give how the mapping of the residual stress component, RS_{xx}, at the lower layers (in $\theta=-45^0$) for antisymmetric lamination varies according to the hole dimensions (a,b). Dimension "a" are selected 0.25xb, 0.5xb, 1xb, 2xb and 4xb although hole dimension b=50mm is constant. As shown in these figures, the plotting of the RS_{xx} is obtained nearly the same. Because all of the lower layers are reinforced under same orientation angle ($\theta=-45^0$). In addition, all of the RS_{xx} values with respect to different hole dimensions are nearly the same because of that the load steps are constant as 100 after loading. It should be taken care the first yield load for a=0.25xb is higher than that for a=4xb.

The distributions of the plastic region at each layer of the antisymmetric ($[45^0/-45^0]_{2)}$ simply supported and clamped laminated plates are presented in Figures 9 and 10, respectively. The plastic regions take place around the hole of the plate for each layer. These regions tended to towards reinforcement direction.. The plastic regions are the same to each other for the adjacent to the midplane due to the woven reinforcement and the loading condition. Namely, the plastic zones at the layer 1 and layer 8 oriented in $45^0$and -45^0, respectively, are completely same. The largest plastic regions appear at the top and bottom layers (layer 1 and layer 8).

The plastic zone formation around the rectangular hole expands as the number of iteration (25, 50, 75 and 100) raises for simply supported plates; the result is presented in Fig 12. In $\theta=45^0$and $\theta=-45^0$ oriented layers, the plastic zones are completely the same either simply supported or clamped plates due to the woven reinforcement. In the simply supported case, the plastic region occurs at the corners in addition to around the rectangular hole with respect to fiber orientation angle. However the region for the clamped case takes place only at the corners of the hole.

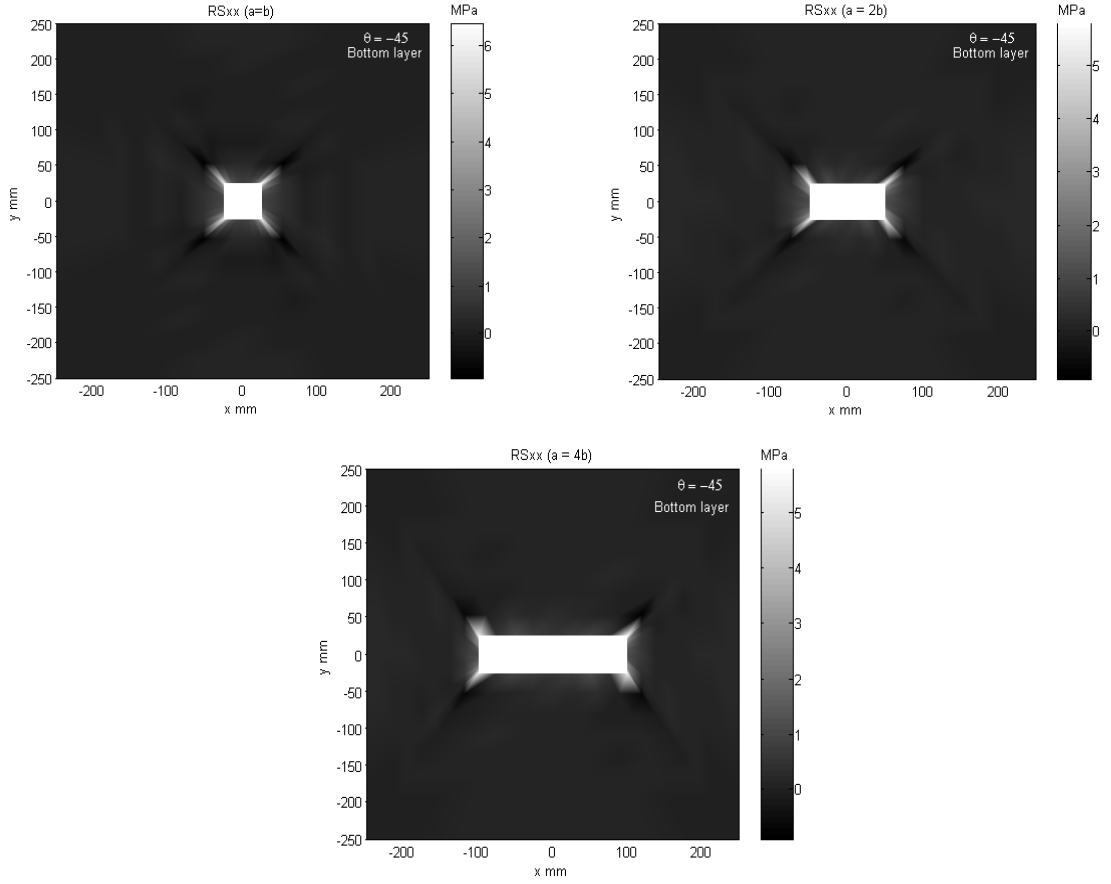

Figure 8:
Mapping of hole dimension (a,b) on the lower surface ($\theta=-45^0$) for antisymmetric clamped laminated plate ($[45^0/-45^0]_2$) and 100 load steps.

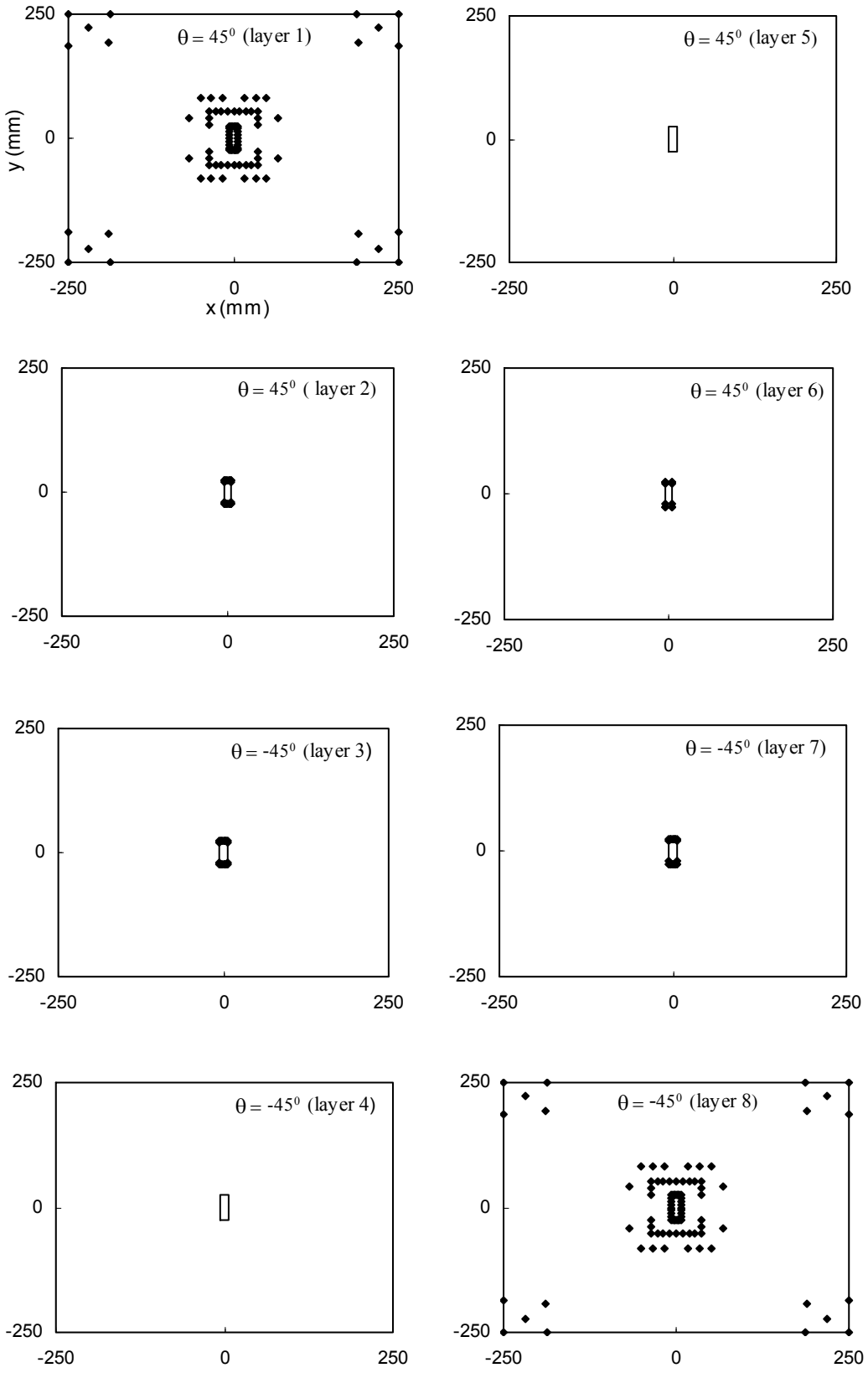

Figure 9:
Nodes in plastic region at each layer for antisymmetric $([45^0/-45^0])_2$ simply supported laminated plates and 100 load steps.

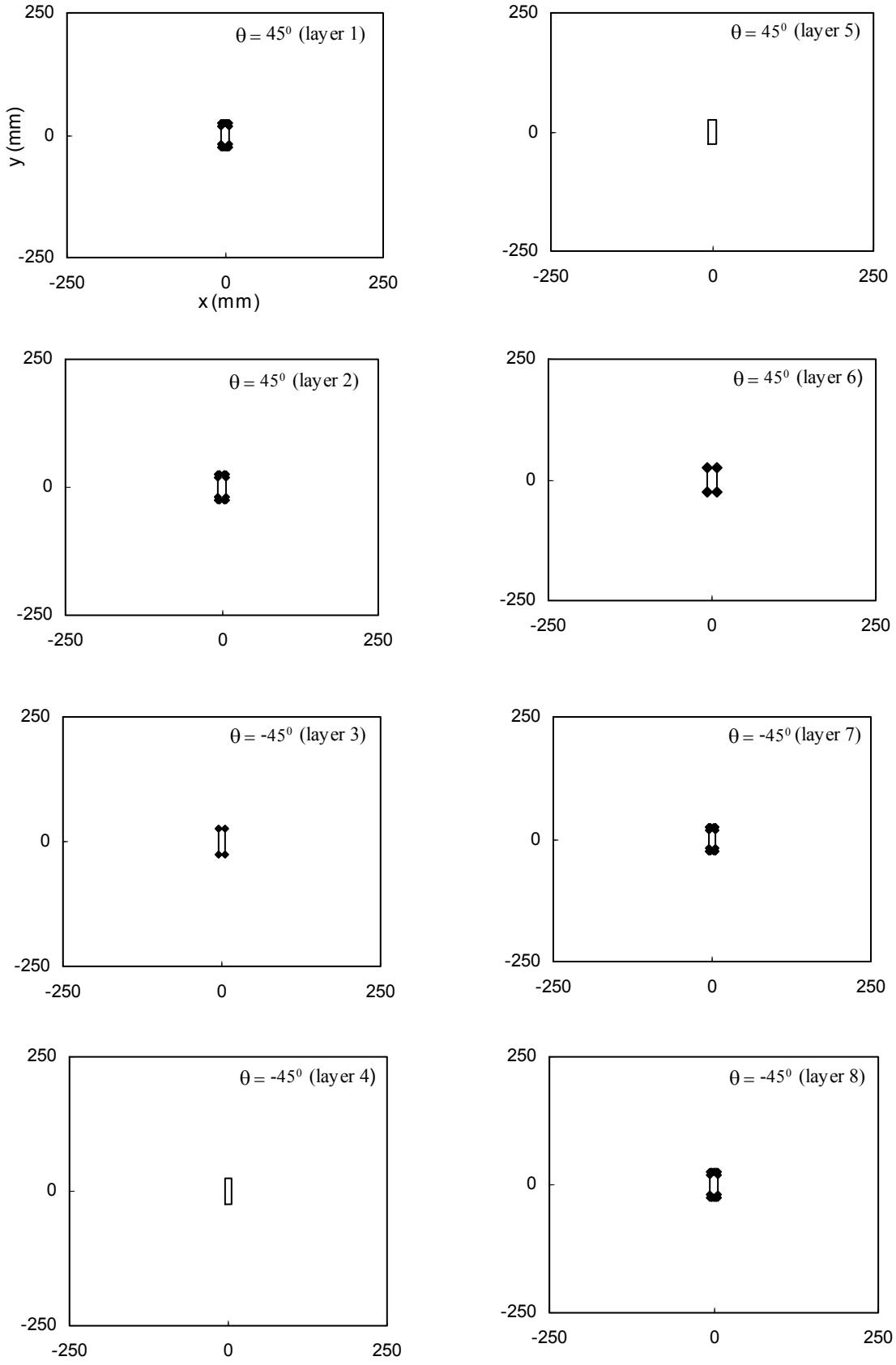

Figure 10:
Nodes in plastic region at each layer for antisymmetric $([45^0/-45^0])_2$ clamped supported laminated plates and 100 load steps.

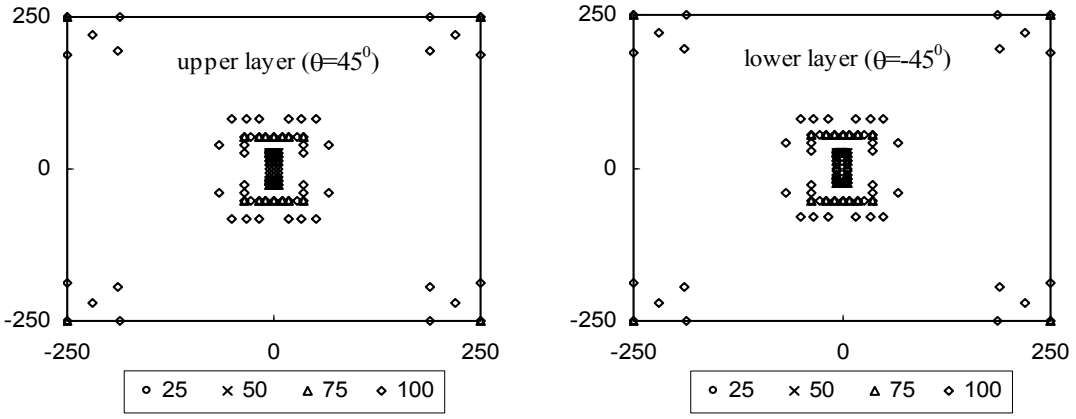

Figure 11:
Variations of plastic zones with load steps (iteration numbers) for simply supported plates ([45⁰/-45⁰]) and antisymmetric lamination.

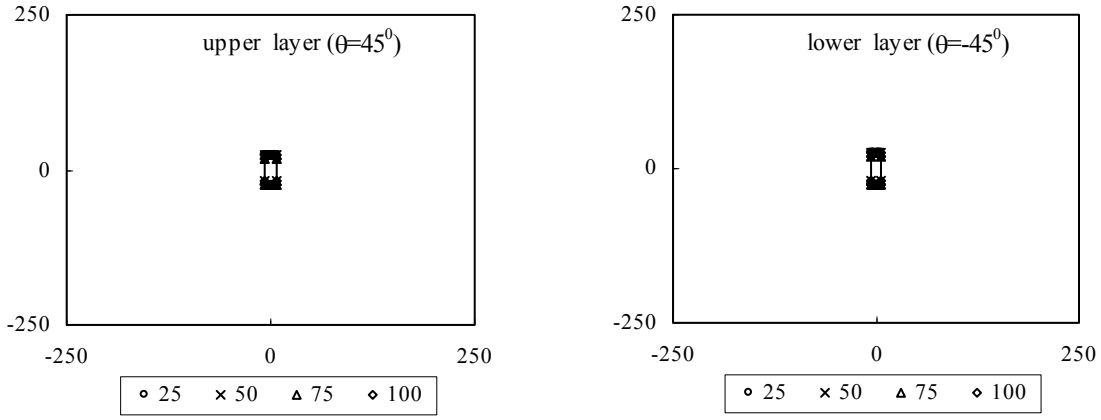

Figure 12:
Variations of plastic zones with load steps (iteration numbers) for clamped plates ([45⁰/-45⁰]) and antisymmetric lamination.

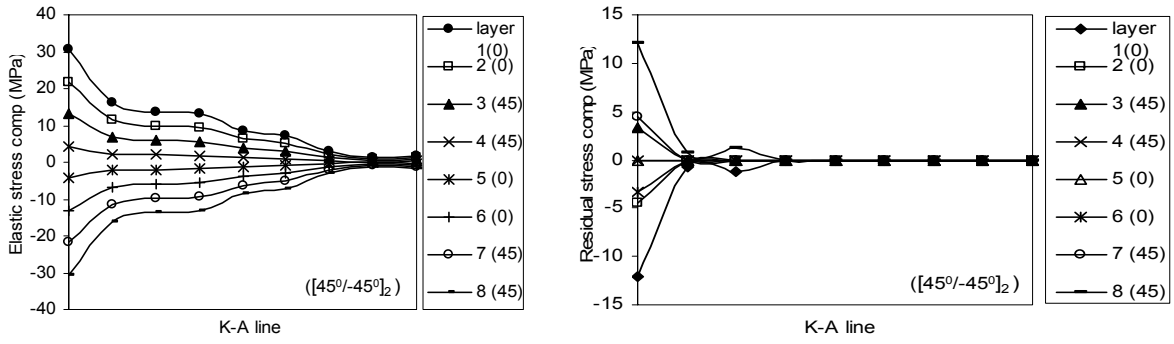

Figure 13:
Elastic (σ_{xx}) and residual stress (RS_{xx}) components on K-A line in antisymmetric ($[45^0/-45^0]_2$) simply supported laminated plate for 100 load steps and each layer.

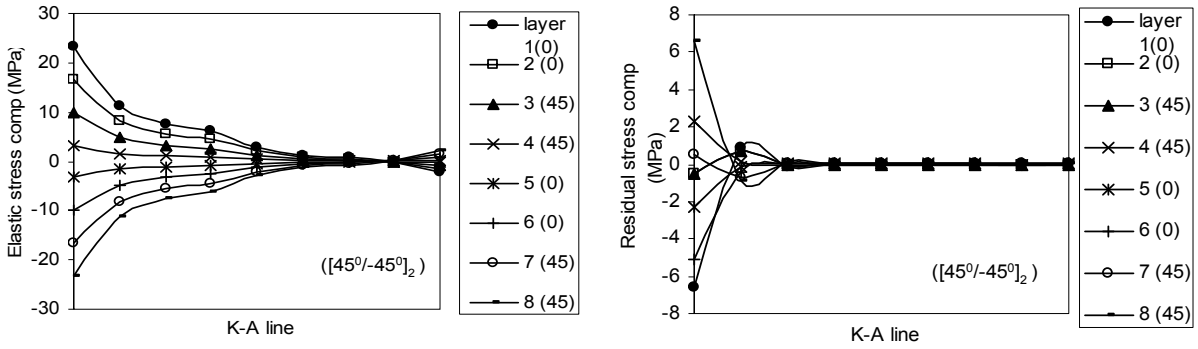

Figure 14:
Elastic (σ_{xx}) and residual stress (RS_{xx}) components on K-A line in antisymmetric ($[45^0/-45^0]_2$) clamped supported laminated plate for 100 load steps and each layer.

Table I. The mechanical properties and yield points of woven reinforced thermoplastic composite layers for diferent materials.

Material	
E_1 (MPa)	9550
E_2 (MPa)	9550
G_{12} (MPa)	670
ν_{12} (MPa)	0.32
X, Axial yield value (MPa)	18.5
Y, Transverse yield value (MPa)	18.5
S, Shear yield value (MPa)	8.26
K, Hardening parameter (MPa) (Plasticity constant)	99.5
n, Strain hardening exponent (-)	0.676
V_f, Fiber volume fraction (-)	0.07

Table II. The uniform transverse force at the yield points of the simply supported and clamped laminated plates for $[\theta^0/-\theta^0]_2$ stacking sequence* (in MPa and axb= 6.25x25 in mm)

Stacking sequence	$[0^0/0^0]_2$	$[15^0/-15^0]_2$	$[30^0/-30^0]_2$	$[45^0/-45^0]_2$
Simply supported				
S	0.00849	0.00890	0.0106	0.01169
AS	0.00849	0.00889	0.0103	0.01170
Clamped				
S	0.02089	0.0206	0.0208	0.0215
AS	0.02089	0.0205	0.0208	0.0215

* S, AS Symmetric and antisymmetric lamination, respectively.

Table III. Maximum elastic and residual stresses components at the corner of the rectangular hole (point K in Fig.1) for all layers in clamped and simply supported laminated plates ($[45^0/-45^0]_2$) for 100 load steps axb= 6.25x25 in mm.

$[(45^0/-45^0])$	Layers	Elastic stresses (MPa)					Residual stresses (MPa)				
		σ_x	σ_y	τ_{xy}	τ_{yz}	τ_{xz}	RS_{xx}	RS_{yy}	RS_{xy}	RS_{yz}	RS_{xz}
(a) Symmetric clamped laminated plates											
Upper layer	1 (45^0)	23.412	22.152	-8.609	0.145	-0.409	-6.608	-6.734	3.123	0.139	0.058
	2 (45^0)	16.723	15.823	-6.149	0.145	-0.409	-0.482	-0.579	0.494	0.169	0.034
	3 (-45^0)	10.034	9.494	-3.689	0.145	-0.409	5.091	5.034	-2.655	0.278	-0.004
	4 (-45^0)	3.345	3.165	-1.230	0.145	-0.409	2.258	2.239	-1.268	0.326	-0.018
	5 (-45^0)	-3.345	-3.165	1.230	0.145	-0.409	-2.258	-2.239	1.268	0.326	-0.018
	6 (-45^0)	-10.034	-9.494	3.689	0.145	-0.409	-5.091	-5.034	2.655	0.278	-0.004
	7 (45^0)	-16.723	-15.823	6.149	0.145	-0.409	-1.379	-1.926	0.940	0.696	-0.510
Lower layer	8 (45)	-23.412	-22.152	8.609	0.145	-0.409	6.608	6.734	-3.123	0.139	0.058
(b) Antisymmetric clamped laminated plates											
Upper layer	1 (45^0)	23.412	22.152	-8.609	0.145	-0.409	-6.608	-6.734	3.123	0.139	0.058
	2 (45^0)	16.723	15.823	-6.149	0.145	-0.409	-0.482	-0.579	0.494	0.169	0.034
	3 (-45^0)	10.034	9.494	-3.689	0.145	-0.409	5.091	5.034	-2.655	0.278	-0.003
	4 (-45^0)	3.345	3.165	-1.230	0.145	-0.409	2.257	2.239	-1.268	0.326	-0.018
	5 (45^0)	-3.345	-3.165	1.230	0.145	-0.409	-2.260	-2.240	1.269	0.326	-0.018
	6 (45^0)	-10.034	-9.494	3.689	0.145	-0.409	-5.092	-5.033	2.654	0.278	-0.003
	7 (-45^0)	-16.723	-15.823	6.149	0.145	-0.409	0.484	0.578	-0.494	0.170	0.034
Lower layer	8 (-45^0)	-23.412	-22.152	8.609	0.145	-0.409	6.613	6.733	-3.123	0.139	0.058
(c) Antisymmetric simply supported laminated plates											
Upper layer	1 (45^0)	30.446	28.796	-10.370	-0.132	-0.713	-12.104	-12.979	4.567	0.609	0.189
	2 (45^0)	21.747	20.569	-7.407	-0.132	-0.713	-4.477	-5.123	1.854	0.620	0.153
	3 (-45^0)	13.048	12.341	-4.444	-0.132	-0.713	3.288	2.907	-1.173	0.707	0.107
	4 (-45^0)	4.349	4.114	-1.481	-0.132	-0.713	6.874	6.746	-3.801	1.154	0.040
	5 (45^0)	-4.349	-4.114	1.481	-0.132	-0.713	-6.887	-6.755	3.806	1.154	0.040
	6 (45^0)	-13.048	-12.341	4.444	-0.132	-0.713	-3.296	-2.904	1.173	0.706	0.107
	7 (-45^0)	-21.747	-20.569	7.407	-0.132	-0.713	4.486	5.123	-1.855	0.620	0.153
Lower layer	8 (-45^0)	-30.446	-28.796	10.370	-0.132	-0.713	12.121	12.983	-4.571	0.609	0.189

Table IV. Maximum elastic and residual stresses components clamped laminated plates ($[\theta^0/-\theta^0]$) for p = 0.0225 MPa constant load.

Layers	Elastic stresses (MPa)					Residual stresses (MPa)				
	σ_x	σ_y	τ_{xy}	τ_{yz}	τ_{xz}	RS_{xx}	RS_{yy}	RS_{xy}	RS_{yz}	RS_{xz}
(a) Maximum stresses at the upper for symmetric laminated plates										
$(0^0/0^0)_2$	22.554	17.074	1.345	1.345	1.248	-1.228	-0.561	0.170	0.033	0.033
$(15^0/-15^0)_2$	22.354	19.187	3.539	1.445	1.337	-2.157	-1.015	0.286	0.039	0.048
$(30^0/-30^0)_2$	19.792	18.463	5.740	1.562	1.447	-1.662	-0.999	-0.522	0.029	0.032
$(45^0/-45^0)_2$	18.341	16.068	6.184	1.617	1.502	-0.903	-0.863	0.372	0.038	0.039
(b) Maximum stresses at the lower for symmetric laminated plates										
$(0^0/0^0)_2$	-22.554	-17.074	-1.345	-1.345	1.248	1.228	0.561	-0.170	0.033	0.033
$(15^0/-15^0)_2$	-22.354	-19.187	-3.539	-1.445	1.337	2.157	1.015	-0.286	0.039	0.048
$(30^0/-30^0)_2$	-19.790	-18.463	-5.740	-1.562	1.447	1.662	0.102	0.522	0.029	0.032
$(45^0/-45^0)_2$	-18.341	-16.068	-6.184	-1.617	1.502	0.903	0.863	-0.372	0.038	0.039
(c) Maximum stresses at the upper for antisymmetric laminated plates										
$(0^0/0^0)_2$	22.554	17.074	1.345	1.345	1.248	-1.228	-0.561	0.170	0.033	0.033
$(15^0/-15^0)_2$	22.589	19.314	3.520	1.438	1.334	-2.240	-1.206	-0.303	0.053	-0.038
$(30^0/-30^0)_2$	20.095	18.382	5.688	1.553	1.443	-1.735	-1.150	-0.509	0.026	0.028
$(45^0/-45^0)_2$	18.341	16.068	6.184	1.617	1.502	-0.903	-0.863	0.372	0.038	0.039
(d) Maximum stresses at the lower for antisymmetric laminated plates										
$(0^0/0^0)_2$	-22.554	-17.074	-1.345	-1.345	1.248	1.228	0.561	-0.170	0.033	0.033
$(15^0/-15^0)_2$	-22.659	-18.895	3.520	-1.438	1.334	2.240	1.206	-0.303	0.053	-0.038
$(30^0/-30^0)_2$	-20.055	-17.169	5.688	-1.553	1.443	1.735	1.150	-0.509	0.026	-0.028
$(45^0/-45^0)_2$	-18.341	-16.068	-6.184	-1.617	1.502	0.903	0.863	-0.372	0.038	0.039

Table V. Maximum elastic and residual stresses components simply supported laminated plates ($[\theta^0/-\theta^0]$) for p = 0.01269 MPa constant load.

Layers	Elastic stresses (MPa)					Residual stresses (MPa)				
	σ_x	σ_y	τ_{xy}	τ_{yz}	τ_{xz}	RS_{xx}	RS_{yy}	RS_{xy}	RS_{yz}	RS_{xz}
(a) Maximum stresses at the upper for symmetric laminated plates										
$(0^0/0^0)_2$	31.942	25.065	0.924	0.278	-0.210	-10.757	-6.490	0.387	-0.166	0.166
$(15^0/-15^0)_2$	28.966	25.095	4.155	-0.174	-0.089	-8.818	-5.970	-0.734	-0.037	0.015
$(30^0/-30^0)_2$	22.372	20.920	6.090	0.075	-0.327	-4.099	-2.807	-1.131	-0.017	0.055
$(45^0/-45^0)_2$	19.247	17.030	-0.344	0.164	0.053	-1.753	-1.678	-0.614	-0.023	0.037
(b) Maximum stresses at the lower for symmetric laminated plates										
$(0^0/0^0)_2$	-31.942	-25.065	0.924	0.278	-0.210	10.757	6.490	-0.387	0.166	-0.166
$(15^0/-15^0)_2$	-28.966	-24.884	-4.155	0.174	0.089	8.818	5.970	0.734	0.037	-0.015
$(30^0/-30^0)_2$	-22.372	-20.920	-6.090	0.075	-0.327	4.099	2.807	1.131	-0.017	0.055
$(45^0/-45^0)_2$	-19.247	-17.030	0.344	0.164	0.053	1.752	1.678	-0.614	-0.023	0.037
(c) Maximum stresses at the upper for antisymmetric laminated plates										
$(0^0/0^0)_2$	31.942	25.065	0.924	0.278	-0.210	-10.757	-6.490	0.387	-0.166	0.166
$(15^0/-15^0)_2$	29.443	25.507	4.208	-0.334	-0.060	-9.309	-5.921	-0.778	0.117	-0.029
$(30^0/-30^0)_2$	22.949	21.240	6.180	-0.065	-0.303	-4.711	-3.165	-1.216	0.011	0.053
$(45^0/-45^0)_2$	19.247	17.030	-0.344	0.164	0.053	-1.753	-1.678	-0.614	-0.023	0.037
(d) Maximum stresses at the lower for antisymmetric laminated plates										
$(0^0/0^0)_2$	-31.942	-25.065	0.924	0.278	-0.210	10.757	6.490	-0.387	0.166	-0.166
$(15^0/-15^0)_2$	-29.443	-25.139	4.208	0.334	-0.060	9.309	5.923	-0.778	-0.117	-0.029
$(30^0/-30^0)_2$	-22.949	-21.243	6.180	0.065	-0.303	4.711	3.165	-1.216	-0.011	0.053
$(45^0/-45^0)_2$	-19.247	-17.030	0.344	0.164	0.053	1.753	1.678	-0.614	0.023	0.037

Fig 13-14 give the elastic and residual stress components at each layer along K-A line for $[45^0/-45^0]_2$ antisymmetric simply supported and clamped plate with rectangular hole (axb=6.25x25 mm) and 100 load steps. At each layer, the maximum stress values are obtained at point K. Because of the uniform transverse load, the stress values at top and bottom layers are higher than those of inner layers. It is obtained that the elastic and residual stresses increase when moving away from the midplane. Because of the $[45^0/-45^0]_2$ lamination and woven fiber type, the stress values are absolutely equal at the couple of layers which have the same distance from the midplane along $\pm z$ direction, in spite of antisymmetric lamination. For example, σ_{xx}=22 MPa and -22 MPa for 2nd and 7th layers, respectively. RS_{xx} values at the mentioned layers are -5 MPa and 5 MPa, respectively. Dispite this situation is also valid for clamped case, the relevant values for clamped case are higher than those for simply supported case. When moving away from K, both of elastic and residual stresses become smaller but only the sign of residual stresses changes within the certain part of K-A line due to the effect of the region where there is no yielding.

7. CONCLUSIONS

The present study shows the stress components and the expansion of the plastic region for the symmetric and antisymmetric simply supported and clamped laminated plates under uniform static transverse loading. The effects of the reinforcement angle on the residual stresses and the plastic zones are obtained in woven-fiber reinforced thermoplastic composite laminated plates. The results can be concluded as below;

- The transverse uniform load values starting the yield have distinct value in small deformation limits for different stacking sequences.
- The yield points of the symmetric oriented plates are higher than those of the antisymmetric plates for both simply supported and clamped cases.
- The yield points of the clamped plates are higher than of simply supported plates.
- The maximum elastic, plastic, and residual stress components are obtained at the top and bottom surfaces for both boundary cases, simply supported and clamped cases.
- The residual stress values for simply supported case are higher than for clamped case.
- Symmetric or antisymmetric lamination due to the loading condition the stress values at the upper and lower layers are higher than at inner layers.

- The plastic regions expand away from the midplane. The largest regions are obtained at the top and bottom surfaces.
- The plastic regions appeared to form in or around the places where the biggest residual stresses took place.
- The plastic regions expand in both symmetric and antisymmetric laminated plates in the direction of fibers around the square hole and the supports for both boundary cases.
- The maximum elastic and residual stress values at $[45^0/-45^0]_2$ stacking sequence are smaller than those at $[0^0/0^0]_2$, $[15^0/-15^0]_2$ and $[30^0/-30^0]_2$ for either symmetric or antisymmetric laminations. In addition, the maximum τ_{xy} values are obtained in $[45^0/-45^0]_2$ orientation angle at lower surfaces for clamped supported.
- The maximum τ_{xy} and RS_{xy} values are obtained in $[30^0/-30^0]_2$ orientation angle at lower and upper surfaces for simply supported.
- When the applied load is increased the plastic regions expand as the number of the yielding nodes increase. This behaviour is obtained for all orientation angles in the simply supported and clamped laminated plates.
- The magnitudes of yield points increase with increasing hole dimensions due to the transverse loading condition.

REFERENCES

1. Karakuzu R., Özel, A. and Sayman, O. (1996) Elastic-Plastic Finite Element Analysis of Metal Matrix Plates with Edge Notches. *Composite Structure* 63(3), 551-558.
2. Arslan, N., Arslan, N. and Okumus, F. (2004) Elastic-Plastic Stress Analysis and Expansion of Plastic Zone in clamped and simply supported thermoplastic-matrix laminated plates with square hole. *Composite Science and Technoogy* 64, 1147-1166.
3. Özcan, R. (2000) Elastic-Plastic Stress Analysis in Thermoplastic Composite Laminated Plates under in-Plane Loading. Composite Structure 49, 201-208.
4. Atas, C. and Sayman, O. (2000) Elasto-Plastic Streess Analysis and Expansion of Plastic Zone in Clamped and Simply Supported Aluminum Metal-Matrix Laminated Plates. *Composite Structure* 49, 9-19.
5. Eijpe, M.I.M, Powell, P.C. (1997) Residual Stress Evaluation in Composite using a Modified Layer Removal Method. *Composite Structure* 37(4), 335-342.
6. Özbay, M. and Ozer, D. (2005) The Analysis of Elasto-Plastic Stresses in The Composite Laminate with a Circular Hole Subjected to In-Plane Loads by Means of Finite Element Method. *J Reinforce Plastic Composite* 24(6), 621-631.
7. Alexandrova, N. and Alexandrov, S. (2004) Elastic-Plastic Stress Distribution in a Rotating Annular Disk. *Mech Base Design of Structur and Mechanic,* 32(1),1-15.
8. Eraslan, A.N. and Akgül, F. (2005) Yielding and Elastoplastic Deformation of Annular Disks of a Parabolic Section Subjected to External Compression. *Turkish J. Enginering Env Science,* 29, 51-60.
9. Arslan, N. and Özben, T. (2005) An Elastic-Plastic Stress Analysis in a Unidirectional Reinforced Steel Fiber Thermoplastic Composite Cantilever Beam Loaded by a Single Force at The Free End, *J Reinforced Plastic Composite,* 24(5), 457-469.
10. Sayman, O. And Sayman, S. (2002) Thermal Elastic-Plastic Stress Analysis of Symmetric Aluminum Metal-Matrix Composite Laminated Plates under Uniformly Distributed Temperature. *J Thermal Stresses*, 25, 363-372
11. Neumann, S., Herrman, P. and Müller WH (2001) Fourier Transforms-An Alternative to Finite Elements for Elastic-Plastic Stress-Strain Analyses of Heterogeneous Materials, *Acta Mechanica*, 149,149-160
12. Arslan, N. (2000) Elasto-Plastic Behavior of Thermoplastic Matrix Plates with Rectangular hole. J Reinforced Plastic Composite, 19(17), 1389-1404.
13. Arslan, N., Celik, M. and Arslan, N. (2002) Prediction of The Elastic-Plastic Behavior of Thermoplastic Composite Laminated Plates ($[0^0/\theta^0]_2$) with Square Hole, *Composite Strucure,* 55, 37-49
14. Sayman, O. Arslan, N. and Pıhtılı, H. (2001) An Elastic-Plastic Stress Analysis in A Thermoplastic Composite Cantilever Beam Loaded Uniformly, *Thermoplasic Composite Material,* 6(14), 523-538.

15. Aktaş, A. (2004) Elastic-Plastic Stress Analysis and Plastic region Expansion of Clamped Aluminum Metal-Matrix Laminated Plates with an Elliptical Hole, *J Reinforced Plastic Composite,* 23(18),1997-2009.
16. Arslan, N., Kaman, M.O. and Duranay, M. (2004) Elastic-Plastic Stress Analysis in Aluminum Metal-Matrix Composite Laminated Plates ($[0^0/\theta^0]_2$) under Transverse Uniformly Distributed Load, *J Reinforced Plastic Composite,* 23 (18), 2025-2045.
17. Yıldız, H., Sayman, O. and Aktaş, M. (2004) Effects of Hardening Parameter and Strain Hardening Exponent on Residual Stress and Plastic Zone Growth in Aluminum Metal-Matrix Composite under Out-of-Plane Loading, *J Reinforced Plastic Composite* 23(18), 2065-2080.
18. Okumus, F. (2005) An Elastic-Plastic Stress Analysis in Silicon Carbide Fiber-reinforced Magnesium Metal-Matrix Composite Beam having Rectangular Cross Section under Transverse Loading, *J Reinforced Plastic Composite*, 24(5), 471- 484.
19. Sayman, O. and Aksoy, S. (2001) Composite Structures, Elastic-Plastic Stress Analysis of Simply Supported and Clamped Aluminum Metal-Matrix Laminated Plates with a Hole. *Composite Structures*, 53, 355-364.
20. Karakuzu, R., Aslan, Z. and Okutan, B. (2004) The Effect of Ply Number, Orientation Angle and Bonding Type on Residual Stresses of Woven Steel Fiber Reinforced Thermoplastic Laminated Composite Plates Subjected to Transverse Uniform Load. *Composite Science and Technology*, (64), 1049-1056
21. Yapici, A., Şahin, Ö.S. and Uyaner, M. (2005) Elastic-Plastic Stress Analysis of Woven Cr-Ni-reinforced Composite-Laminated Plates with a Hole under in-Plane Loading. *J Reinforced Plastic Composite,* 24(5), 503-511.
22. Bahei-El-Din, Y.A. and Dvorak, G.J. (1982) Plasticity Analysis of Laminated Composite Plates, *Transactions of The Asme,* 49, 740-746.
23. Gibson, F.R. (1994) Principles of Composite Material Mechanics. McGraw-Hill International Editions.
24. Bathe, K.J. (1982) Finite Element Procedures in Engineering Analysis. Prentice-Hall Inc., Englewood Cliffs, New Jersey.
25. Mohr GA (1992) Finite Elements for Solids, Fluids and Optimization. Oxford University Press, Oxford.
26. Johnson, W.and Mellor, P.B. (1983) Engineering Plasticity, JohnWiley&Sons, New York.

Makale 03.02.2009 tarihinde alınmış, 23.08.2010 tarihinde düzeltilmiş, 26.08.2010 tarihinde kabul edilmiştir. İletişim Yazarı: T. Özben (tamoz@dicle.edu.tr).